Parameter Optimization of a Tubular Linear Type Reluctance Motor for High Thrust Force

M.M.Ghazaly, C.K.Yeo, S.H.Chong, I. Yusri, S.P.Tee

Centre of Excellence of Robotics & Industrial Automation (CeRIA), Faculty of Electrical Engineering,
Universiti Teknikal Malaysia Melaka
mariam@utem.edu.my

Abstract—**In this paper, the parameters of a linear type reluctance motor was verified by varying the motor parameters; i.e. (a) air gap thickness and (b) number of winding turns of a 3-phase Tubular Linear Reluctance Motor (TLRM). The aim is to optimize the electromagnetic thrust force. At first, a three-dimension TLRM structure is designed using ANSYS Maxwell 3D software Ver. 17.2. Next, the effects of the varying parameters are evaluated using Finite Element Method (FEM) analysis. The obtained results show that the variation of the air gaps and the number of winding turns greatly influence the electromagnetic thrust force. It is found that the maximum thrust force of the design TLRM is 370.3mN at 0.5mm air gap thickness and 300 numbers of winding turns.**

Index Terms—**Finite Element Method (FEM); Linear Electromagnetic Motor; Thrust Force; Tubular Linear Reluctance Motor.**

I. INTRODUCTION

Electric linear motors are known as the best candidate to replace the conventional rotary-to-linear motor for the linear motion drive, as it does not require additional mechanism such a gear and ball-screw to translate a rotary motion to the linear motion. There are various types of electric linear motors, such as piezoelectric motor, electrostatic motor and electromagnetic motor [1]–[3]. The characteristic differences of these electric linear motors are the working range, the heat dissipation and the thrust force as shown in Table 1. The electromagnetic motor has the advantages of long working range and large thrust force but it still has disadvantage which is it has high heat dissipation compared to the other electric motors [4].

Table 1
General Characteristic of Electric Motors.

Type of Motor	Characteristic			
	Working Range	Thrust Force	Drive complexity	Heat Dissipation
Piezoelectric	Short	High	Moderate	Nonlinear
Electrostatic	Short	Small	Moderate	Nonlinear
Electromagnetic	Long	High	Complex	Nonlinear

There are few types of linear electromagnetic motors; i.e. Linear Permanent Magnet (LPM) motor and Linear Reluctance (LR) motor. The LPM motor is widely used in high precision motors, robotic and biomedical industry since as it has high power density and high precision [5]–[10]. LPM motor uses permanent magnet which may lead to higher cost especially when neodymium magnet is implemented. An alternate candidate for replacing the LPM motor is the Linear Reluctance Motor (LRM). Both LPM and LRM consist of two main parts; the stator that consists of coil windings and the rotor or mover. The main difference between these two motors is the LPM motor has permanent magnet on the mover structure while the LRM does not require permanent magnet on the mover structure. The LRM consists of two main materials; i.e.: (i) ferromagnetic material for the both stator and rotor core and (ii) copper for the winding coil. Due to the lack of magnetic field source of the permanent magnet, the LRM is not able to produce high thrust density as compared to the LPM motor. The LRM can be designed either in a flat shape or in a tubular shape. The tubular shape of LRM is commonly known as Tubular Linear Reluctance Motor (TLRM). Comparison between the tubular shape and the flat shape is the coil winding in the tubular shape of the LRM does not require the end windings as the flat shape does. The coils end winding can reduce the efficiency of the motor. All coils in the TLRM are active participants in the magnetic field and the thrust production [11–16].

In this paper, a new design of TLRM is evaluated for determining the maximum thrust force characteristics when the air gap thickness between the stator and the mover and the number of coil winding turns are varied. The analysis is done using ANSYS Maxwell 3D software Ver. 17.2 and using Finite Element Method (FEM) analysis [17]–[20].

II. TLRM DESIGN STRUCTURE GEOMETRIES

In this paper, the TLRM is design based on the following performance specifications; which are to design a miniature size TLRM that has a long working range (i.e: 100 mm displacement), but at the same time it is able to produce high thrust force (i.e.: 20 N). To evaluate the FEM analysis, the TLRM is drawn using ANSYS Maxwell 3D software Ver. 17.2. The TLRM consists of two main structures, the stationary part (stator) that contains coil phase windings and the mover part (rotor). Figure 1 (a) shows the construction of the TLRM. The isometric cross section view of the TLRM is shown in Figure 1 (b). The three identical coils phase winding sets are connected in series connection to each phase and driven by an external input current amplifier. The stator and the rotor are constructed using ferromagnetic material and both have the teeth shape design. Figure 2 illustrates the dimensions of the proposed TLRM and the details of the initial parameters are summarized in Table 2.
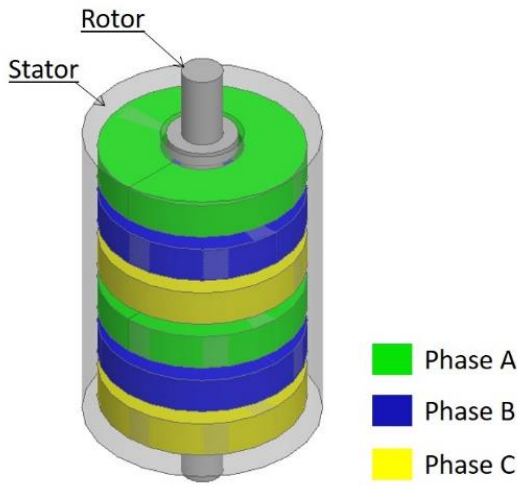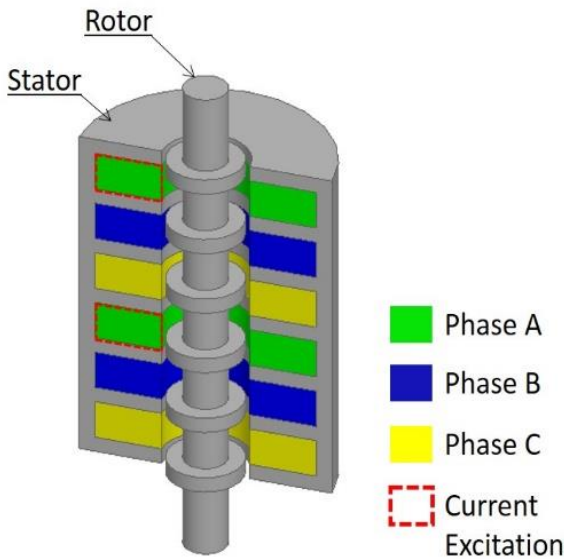
Figure 1: (a) TLRM Isometric View

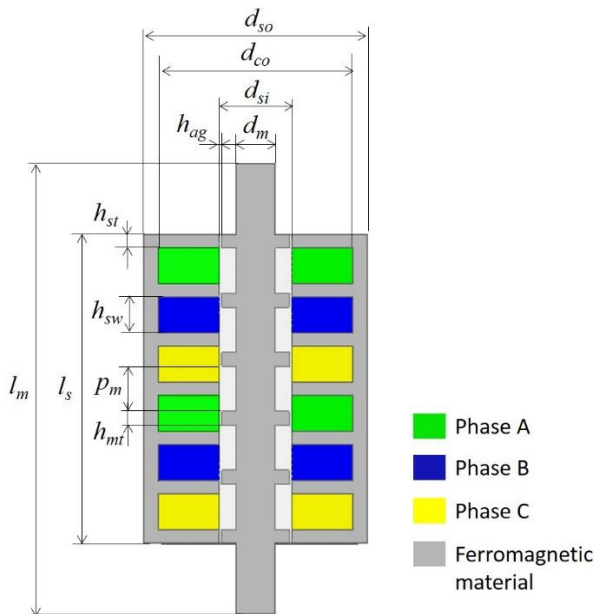Figure 1: (b) TLRM Isometric Cross Section

Figure 2: TLRM Isometric Cross Section

Table 2
TLRM Initial Parameter

Initial Parameter	Dimension (mm)
Stator outer diameter, d_{so}	63
Stator inner diameter, d_{si}	20
Stator tooth width, h_{st}	10
Stator slot width, h_{sw}	4
Stator length, l_s	88
Coil outer diameter, d_{co}	27.5
Mover diameter, d_m	11
Mover tooth width, h_{mt}	4
Mover tooth pitch, p_m	14
Mover length, l_m	128
Air gap thickness, h_{ag}	0.5

The electromagnetic force, F is derived from the rate of change of co-energy with mover position shown by Eq. 1;

$$F(i,z) = \frac{\partial W'(i,z)}{\partial x} \qquad (1)$$

Where $W'(i,z)$ is magnetic co-energy at position z and current i, which it can be derived from the coil flux-linkage, $\varphi(Wbt)$. $\varphi(Wbt)$ is a function of current and mover displacement, given by Eq. 2;

$$W(i,z) = \int_0^i \varphi(z,i)\,di \qquad (2)$$

III. FINITE ELEMENT METHOD ANALYSIS RESULTS

A. Magnetic Field Distribution

The Finite Element Method (FEM) analysis for the TLRM magnetic field distribution was performed using ANSYS Maxwell 3D software Ver. 17.2. FEM analysis is a computerized method for predicting the TLRM reaction to real-world thrust forces and magnetic field distribution.The input current used in this analysis are varied from 0 A to 2 A with the interval of 0.2 A. From the result of magnetic field distribution, when the input current is excited at phase A and phase A', the magnetic flux flows from the stator teeth to the mover teeth as illustrated in Figure 3.

B. Varying Air Gap Thickness

In order to obtain the maximum thrust force of the motor, the air gap thickness and the number of winding turns are varied. The air gap thickness is varied from 0.5 mm to 1.5 mm with the interval of 0.2 mm while the parameter of the winding turns is 100 turns. Figure 4 shows the example of the air gaps variation between 0.5 mm, 0.9 mm and 1.5 mm. The computed thrust forces gradually increased which correspond to the input current as shown in Figure 5. The maximum of 42 mN thrust force can be obtained with the smallest air gap thickness of 0.5 mm. The largest air gaps thickness, i.e. 1.5 mm produced the smallest thrust force value of 6.4 mN. As the thickness of the air gap becomes smaller, the reluctance of the air gap becomes small and the thrust force becomes larger. It can be depicted that, as the size of the air gap thickness decreases, the reluctance of the air gap decreases, thus increasing the electromagnetic force.
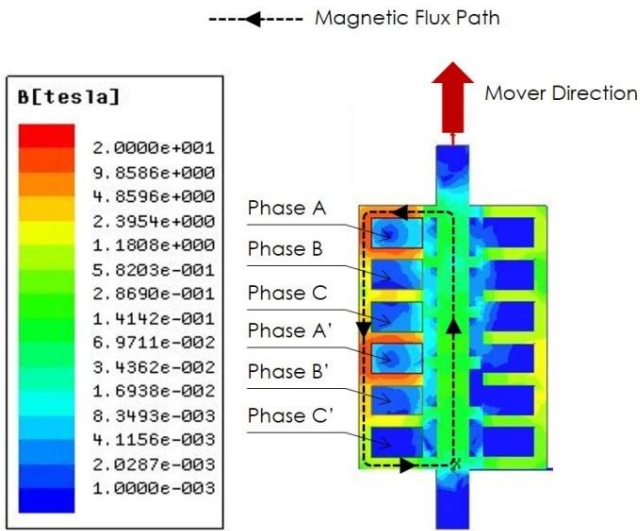
---- ◄---- Magnetic Flux Path

Figure 3: Magnetic Flux Density

.

Air gap thickness,
h_{ag} = 0.5 mm h_{ag} = 0.9 mm h_{ag} = 1.5 mm
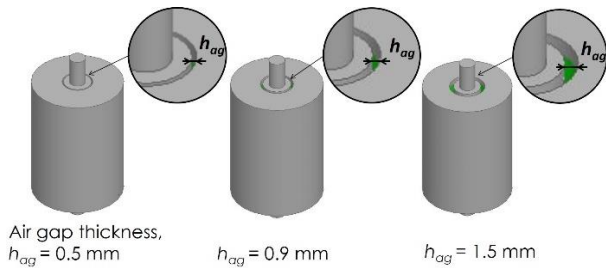
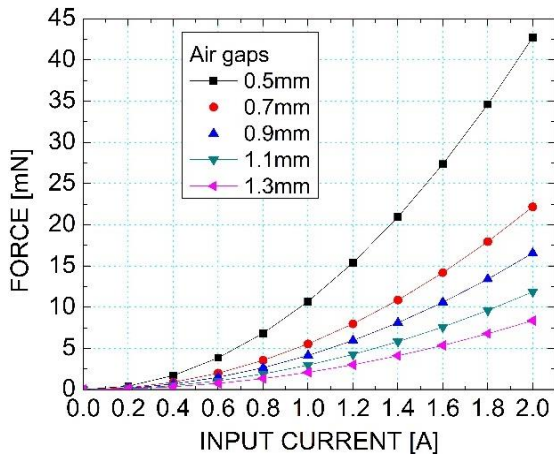Figure 4: Structure Comparison When Air Gaps Are Varied

Figure 5: Varying Of Air Gaps Thickness

C. Varying Number Of Windings Turns

The number of winding turns is varied from 100 turns to 300 turns with the interval of 50 turns while the air gap, i.e. 0.5 mm remained constant. From Figure 6, it can be depicted that the highest number of winding turns i.e. 300 turns generate the highest thrust force of 370.3 mN. The minimum thrust force 42 mN was produced by the 100 turns. It can be concluded that as the number of winding turns increases, the thrust force also increased. This circumstance is expected

since as the number of winding turns increase, the concentrated current at the coil become larger hence increasing the magnetic fields subsequently generating more electromagnetic force.
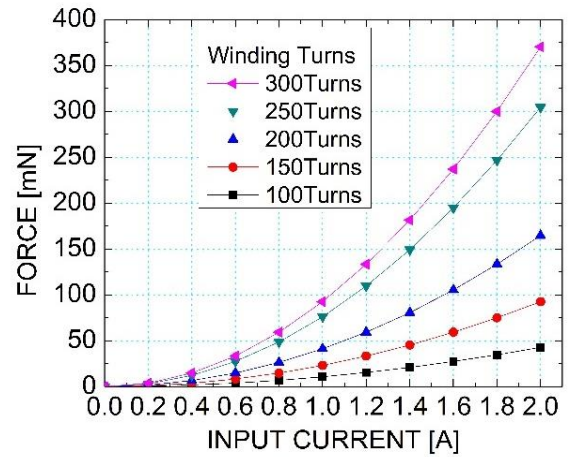

Figure 6: Varying Of Number Winding Turns

IV. CONCLUSIONS

The thrust force characteristics of the varying air gap and the varying number of winding turns are presented in this paper. The simulation results of FEM analysis have shown that the air gap thickness and the number of winding turns influence the thrust force of the TLRM. For the air gap variance, the smaller the gap will contribute higher thrust force. For the number of winding turns, the higher the number of winding turns will generate higher thrust force. The optimum parameters of the varying parameter are shown in Table 3. These optimum design parameters will be used in the motor fabrication which is the next step of this research work. The comparison between the experimental result and simulation result will be done to clarify the results.

Table 3: TLRM Optimize Parameters

No	Varying Parameter	Optimum Parameter	Thrust force
1	Air Gap Thickness	0.5 mm	42 mN
2	Number of Winding Turns	300 turns	370.3 mN

REFERENCES

[1] H. J. M. T. A. Adriaens, W. L. de Koning, and R. Banning, "Modeling piezoelectric actuators," *IEEE/ASME Trans. Mechatronics*, vol. 5, no. 4, pp. 331–341, 2000.

[2] M. M. Ghazaly, L. T. Kang, C. Y. Piaw and K.Sato., "Force Optimization of an Force Artificial Muscle Actuated Underwater Probe System using Linear Motion Electrostatic Motor," *J. Teknologi*, vol. 9, no. 2, pp. 113–118, 2015.

[3] M. Markovic, M. Jufer, and Y. Perriard, "Analytical force determination in an electromagnetic actuator," *IEEE Trans. Magn.*, vol. 44, no. 9, pp. 2181–2185, 2008.

[4] M. M. Ghazaly and K. Sato, "Basic characteristics of a multilayer thin electrostatic actuator supported by lubricating oil for a fine-motion stage," *Precision. Engineering*, vol. 36, no..1, pp. 77–83, 2012.

[5] J. Ji, Z. Ling, J. Wang, W. Zhao, G. Liu, and T. Zeng, "AU-03 Design and Analysis of a New Halbach Magnetized Magnetic Screw for Artificial Hearts.," *IEEE Trans. Magn.*, vol. 47, no. 10, p. 4480, 2015.

[6] K. min Lee, Y. Kim, J. K. Paik, and B. Shin, "Clawed Miniature Inchworm Robot Driven by Electromagnetic Oscillatory Actuator," *J. Bionic Eng.*, vol. 12, no. 4, pp. 519–526, 2015.

[7] S. C. Shen, Y. J. Wang, and M. T. Shih, "A novel dual-screen projection system using a balance-type micromirror with a piezoelectric actuator," *Sensors Actuators, A Phys.*, vol. 199, pp. 80–88, 2013.

[8] J. Ponmozhi, C. Frias, T. Marques, and O. Frazao, "Smart sensors/actuators for biomedical applications: Review," Meas. *J. Int. Meas. Confed.*, vol. 45, no. 7, pp. 1675–1688, 2012.

[9] S. C. Chen, H. Choi, P. T. C. So, and M. L. Culpepper, "Thermomechanical actuator-based three-axis optical scanner for high-speed two-photon endomicroscope imaging," *J. Microelectromechanical Syst.*, vol. 23, no. 3, pp. 570–578, 2014.

[10] O. Felfoul, A. Becker, C. Bergeles, and P. E. Dupont, "Achieving Commutation Control of an MRI-Powered Robot Actuator," *IEEE Trans. Robot.*, vol. 31, no. 2, pp. 387–399, 2015.

[11] N. Bianchi, S. Bolognani, D. D. Corte, and F. Tonel, "Tubular Linear Permanent Magnet Motors: An Overall Comparison," *IEEE Trans. Ind. Appl.*, vol. 2, no. 2, pp. 1266–1273, 2002.

[12] Z. Q. Zhu and D. Howe, "Halbach permanent magnet machines and applications : a review," IEE Proc. - Electr. Power Appl., vol. 148, no. 4, pp. 299–308, 2001.

[13] B. Lequesne and S. Member, "Permanent Magnet Linear Motors for Short Strokes," *IEEE Trans. Ind. Appl.*, vol. 32, no. 1, pp. 161–168, 1996.

[14] J. F. Pan, Y. Zou, and G. Cao, "An Asymmetric Linear Switched Reluctance Motor," *IEEE Trans. Energy Convers.*, vol. 28, no. 2, pp. 444–451, 2013.

[15] B. M. Dutoit, P. A. Besse, and R. S. Popovic, "Planar multidipolar electromagnetic actuators," *IEEE Trans. Magn.*, vol. 39, no. 2 II, pp. 1026–1034, 2003.

[16] S. Gibson, G. W. Jewell, and R. E. Clark, "Variable-airgap, cylindrical, linear variable reluctance actuators for high-force, medium-stroke applications," *IET Electr. Power Appl.*, vol. 3, no. August 2006, p. 352, 2009.

[17] J. Lee, E. M. Dede, D. Banerjee, and H. Iizuka, "Magnetic force enhancement in a linear actuator by air-gap magnetic field distribution optimization and design," Finite Elem. Anal. Des., vol. 58, pp. 44–52, 2012.

[18] S. Suzuki, Y. Kawase, T. Yamaguchi, S. Kakami, K. Hirata, and T. Ota, "Dynamic Analysis Method of Spiral Resonant Actuator Using 3-D FEM," *IEEE Trans. Magn.*, vol. 46, no. 8, pp. 3157–3160, 2010.

[19] A. di Gaeta, L. Glielmo, V. Giglio, and G. Police, "Modeling of an electromechanical engine valve actuator based on a hybrid analytical - FEM approach," *IEEE/ASME Trans. Mechatronics*, vol. 13, no. 6, pp. 625–637, 2008.

[20] K. Tani, T. Yamada, and Y. Kawase, "Dynamic Analysis of Linear Oscillatory Actuator Driven by Voltage Source Using FEM with Edge Elements and 3-D Mesh Coupling Method," *IEEE Trans. Magn.*, vol. 36, no. 4(1), pp. 1826–1829, 2000.